Calculating Combined Amplitude and Phase Modulated Power Signal Parameters

Gerard N. Stenbakken, *Life Member, IEEE*

Abstract— **The ability to monitor and control the dynamics of the electric power grid is important. That is why the proposed revision to the IEEE Synchrophasor Standard IEEE C37.118 adds dynamic performance requirements. One of the new requirements is expected to be for accurate phasor and frequency measurements with a specified level of combined phase and amplitude modulation of the power signals. This paper describes the equations for this type of modulation. Direct solutions are developed for calculating the modulation parameters from measurements of the fundamental and first order sidebands of the modulated signal. These components can be determined by a Fourier transform of the signals. This analysis will help with the calibration of PMUs and the calibration of PMU calibrators generating such test signals.**

***Index Terms*—Amplitude Modulation, Calibration, Demodulation, Frequency Modulation, Phase Modulation, Phasor Measurement Units.**

I. Introduction

The U.S. electric power grid is being modernized to accommodate more distributed power sources and to be able to transmit that power long distances to major loads. To keep such an evolution from destabilizing the grid, the grid controls systems are incorporating more instruments to monitor the state of the grid. The instruments that provide significant observability of the grid are Phasor Measurement Units or PMUs. These instruments monitor the state of the grid at a single point and transmit the magnitude and phase of the point in real time to control centers or other instruments. The high data rate of these instruments, 30 to 60 or more readings per second, allow the monitoring of grid dynamics. Many papers cover the use of PMUs to monitor grid dynamics [1]-[4]. These instruments are able to measure the modulation of the electric power signals and measure the magnitude and damping of these oscillations [5]-[9]. Electric utilities are installing significant numbers of these instruments throughout the power grid.

To provide phase angles that apply across a power grid, PMUs measure phase angles relative to a nominal cosine wave at 50 Hz or 60 Hz synchronized to coordinated universal time (UTC). These phase angles are referred to as absolute phase angles. PMUs generally make use of clocks synchronized to the global positioning system (GPS) to reference UTC.

The current standard that defines the performance of PMUs is IEEE Standard for Synchrophasors for Power Systems, C37.118-2005 [10]-[12]. When this standard was developed there was not general agreement on the dynamic performance requirements for PMUs. The standard only defines PMU performance for steady state conditions. That standard is being revised and is expected to incorporate a number of dynamic requirements.

Tests to verify the performance of PMUs have been developed [13]-[16]. Some of these tests cover dynamic conditions [17]-[21] as well as steady state testing. This paper focuses on one of the new requirements proposed for PMUs: the testing of the PMU's errors during simultaneous amplitude and phase modulation of the power signals. Previous analysis of these signals made use of decomposing this combination of modulations into three phase-modulated signals [22]. This approach was used to develop testing algorithms for PMUs with modulated signals. The equations developed in this paper will allow a quicker solution of the modulation parameters than that approach.

There is a need for methods appropriate for calibrating PMU calibrators. Such methods must be more accurate than the PMU calibrators and cover the signal types that are expected to be required by the updated Standard. Calibration of PMU calibrators requires that the signals they generate be measured and the accuracy of the calibrators verified. The new standard is also expected to have requirements for the frequency and rate of change of frequency (ROCOF) measured by PMUs during this combined modulation.

This paper describes a method for analyzing such power signals and determining accurate estimates of the phasors, frequency, and ROCOF. Amplitude modulation of a sine wave generates two sidebands with frequencies above and below the fundamental signal frequency. Phase modulation generates a large number of sidebands. The method developed in this paper uses measurements of the power signal over one cycle of the modulation. This data is analyzed to determine the magnitudes and phases of the fundamental and first two sidebands. These six values are used to estimate the modulation parameters and from those values to estimate the dynamic and steady state phasor, frequency, and ROCOF values.

Section 2 of this paper describes the basic equations for modulated power signals, and section 3 describes the method for analyzing a modulated signal from samples. The sections following those describe the modulation equations, an approximate solution for the modulation parameters, a higher accuracy solution for the modulation parameters, and the

This work was supported by a contract from Fluke Corporation, a subsidiary of the Danaher Corporation, Everett, WA.

G. N. Stenbakken is with GNS Consulting, Potomac, MD 20854 USA (email: gstenbakken@nist.gov).

978-1-4577-1002-5/11/$26.00 ©2011 IEEE

accuracy of these solutions for estimating the phasors, frequency, and ROCOF. This method provides an accurate method for calibrating PMU calibrators generating combined modulated signals.

II. Modulated Signals

PMUs typically measure three-phase voltage and current signals. They can output the individual phasors or the positive, negative, and zero sequence phasors of the voltages and currents. They also output the signal frequency and ROCOF values. The sequence values can be determined from the three individual phasor values. The method for determining the phasors for each of the three phases are identical. In this paper we examine only the method for determining the parameters of a modulated phase A voltage signal. The equation for phase A voltage X_a with a combined amplitude and phase modulation is given by

$$X_a = X_m\left[1 + k_x\cos(\omega t + \varphi)\right]\cos\left[\omega_0 t + k_a \sin(\omega t + \theta)\right], \quad (1)$$

where X_m is the magnitude of the fundamental signal, k_x is the amplitude modulation index, φ is amplitude modulation phase angle, ω is the modulation frequency, t is time, ω_0 is the frequency of the fundamental in radians per second, k_a is the phase modulation index, and θ is the phase modulation phase angle. The frequencies of the amplitude and phase modulations are considered the same. Their phases may be different. Since the PMUs and the test systems are synchronized to UTC, we assume that the time, modulation frequency, and fundamental frequency are known.

Equation (1) is a general form of the combined modulation equation that allows for variable phase angles of the modulations at the start of the window, for example at time $t = 0$, and allows the two modulations to have different phases. This is necessary if these equations are to be used to fit arbitrary combined modulation signals. The proposed revision to C37.118 gives specific equations for each of the three-phase combined modulation waveforms. The equation for phase A is

$$X_a = X_m\left[1 + k_x\cos(\omega t)\right]\cos\left[\omega_0 t + k_a \cos(\omega t - \pi)\right]. \quad (2)$$

This is the special form of (1) with amplitude modulation phase $\varphi = 0$ and phase modulation phase $\theta = -\pi/2$.

The PMU measures one of two phasors for modulated signals. The PMU calibrator must be able to determine both of these and select the correct one to use as a reference depending on the relation between the PMU's reporting rate and the modulation frequency. As an example, consider testing a PMU with a power signal that is phase modulated at a frequency of 5 Hz. If the PMU is set for a reporting rate of 60 frames per second, the PMU phasor values and frequency are compared to the dynamic phasors and frequency reference values that are changing at the modulation rate of 5 Hz. The errors in this comparison are part of the measurements used to determine the bandwidth of the PMU. However, if the PMU is set to a reporting rate of 10 frames per second, the PMU phasor values and frequency are compared to the steady-state or fundamental phasors and frequency reference values that are not changing. The errors in this comparison are part of the measurements used to determine the out-of-band interference rejection of the PMU. Since the modulation is at the Nyquist frequency for the 10 frames per second reporting rate the PMU must filter out the modulation.

Thus, if the modulation frequency is low the PMU is expected to report the dynamic phasor accurately for power signals with very low modulation frequencies up to the required bandwidth limit frequency. For modulation frequencies above the required bandwidth limit up to half the reporting rate is a transition region with no phasor or frequency accuracy requirements. For modulation frequencies greater than half the reporting rate, the PMU must report the steady state phasor. The steady state phasor is constant in time, showing no amplitude or phase variation at the modulation frequency. For calibration purposes we need to know the dynamic phasor, frequency, and ROCOF and the steady state phasor values for a modulated signal.

The dynamic phasor for X_a from (1) at time $t = 0$ is a vector with a magnitude and angle of

$$\vec{X}_a = X_m\left[1 + k_x\cos(\varphi)\right] \angle k_a \sin(\theta). \quad (3)$$

Absolute phase angles are defined relative to a nominal cosine wave that is oscillating at the nominal system frequency of 50 Hz or 60 Hz. Let ω_n be the nominal system frequency in radians per second. At the start of the current UTC second let ξ_c be the absolute phase angle of the signal fundamental, φ_c be the amplitude modulation phase angle, and θ_c be the phase modulation phase angle. For time $t = t_1$ relative to the start of the current UTC second the dynamic synchrophasor is

$$\begin{aligned}\vec{X}_a = {} & X_m\left[1 + k_x\cos(\omega t_1 + \varphi_c)\right] \\ & \angle\left(\xi_c + (\omega_0 - \omega_n)t_1 + k_a\sin(\omega t_1 + \theta_c)\right). \end{aligned} \quad (4)$$

The frequency of the dynamic phasor f_D is the rate of change of the dynamic phase angle independent of ω_n and is given by

$$f_D(t_1) = \omega_0 + k_a\, \omega\, \cos(\omega t_1 + \theta_c). \quad (5)$$

The rate of change of frequency *ROCOF* is the derivative of the frequency and is given by

$$ROCOF_D = -k_a\, \omega^2\, \sin(\omega t_1 + \theta_c). \quad (6)$$

The steady-state phasor for time $t = 0$ is the sum of two vectors given by

$$\vec{X}_{a0} = X_m J_0(k_a) \angle\, 0 + X_m k_x J_1(k_a) \sin(\varphi - \theta) \angle -\frac{\pi}{2}, \quad (7)$$

where $J_n(k_a)$ is the n^{th} order Bessel function of the first kind. The frequency of the steady state phasor is $f_S = \omega_0$ and $ROCOF_S$ is 0. The derivation of these equations is described below.

Equation (7) indicates that the magnitude and phase of the fundamental changes with the difference between the amplitude and phase modulation angles, φ and θ. The performance requirements of the proposed C37.118.1 standard revision is expected to require accurate phasors in the presence of modulations with amplitude and phase modulation indexes of 0.1. With these modulation indexes, a combined modulation gives a negligible fundamental magnitude change, but a phase change that is dependent on the difference between the amplitude and phase modulation angles. This difference has a maximum angle change of about 0.005 rad or 0.29°. Without considering the analysis in this paper, one could easily assume that the phase of the steady-state phasor is the same as the unmodulated phasor. This assumption is true for amplitude or phase modulations individually. This assumption could make a worst case phase error that results in a total vector error [10], TVE, of about 0.5% for a combined modulation. This is a significant error contribution, since the standard requires the PMUs to have a TVE of less than 1%. TVE is a measure of the combination of magnitude and phase angle errors combined in quadrature.

III. Analysis Method

The analysis method for measuring the modulation parameters of a signal consists of sampling the modulated signal over an integer number of cycles n of the modulation. That is, the sampling is done over a time window T_W of length $T_W = n\ 2\ \pi/\omega$. The assumption is made that the fundamental frequency ω_0 is related to the modulation frequency such that there is an integer m such that $m/\omega_0 = n/\omega$. Thus, an integer number of fundamental cycles and an integer number of modulation cycles fit into the same sampling window, T_W.

Sample the modulated power signals over a window T_W starting on a UTC second. The sampling rate must be at least three times the fundamental frequency in Hz, i.e., $> 3\ \omega_0/(2\ \pi)$. Let the samples be $x(t_i)$ and the vector of samples be given by $X(T_W)$. Let the Fourier transform of $X(T_W)$ given by $\mathcal{F}(X(T_W))$ be the magnitude and phases of the Fourier components. Then the m[th] Fourier component $\mathcal{F}_{\mathrm{m}}$ is the measurement estimate of the fundamental component and the component $\mathcal{F}_{\mathrm{m+bn}}$ is the b[th] upper sideband vector estimate and $\mathcal{F}_{\mathrm{m-bn}}$ is the b[th] lower sideband vector estimate.

This same analysis method was used on simulated signals to validate the equations given below as the derivation of the equations for this paper was carried out. This analysis will be used on measured signals to derive estimates for the vectors of the fundamental and sidebands of the modulated signal and used to estimate the modulation parameters.

Now the equations for modulated signals will be given so the relation between the Fourier components of a modulated signal and the modulation parameters can be derived.

IV. Modulation Equations

A. Amplitude modulation

Using the parameters defined in section 2 the formula for amplitude modulation is given by

$$X_a = X_m\left[1 + k_x \cos(\omega t + \varphi)\right]\cos(\omega_0\, t). \tag{8}$$

Amplitude modulation of a signal gives the fundamental and two sidebands as shown by the expansion of (8) as

$$\begin{aligned} X_a = {} & X_m \cos(\omega_0\, t) + X_m \tfrac{k_x}{2}\cos[(\omega_0 + \omega)t + \varphi] \\ & + X_m \tfrac{k_x}{2}\cos[(\omega_0 - \omega)t - \varphi]. \end{aligned} \tag{9}$$

The fundamental has the same magnitude and phase as the unmodulated signal and the sidebands have magnitudes of half the modulation index times the magnitude of the fundamental. Thus, for a modulation index of 0.1 the sidebands each have magnitudes of 0.05 times the magnitude of the fundamental. The upper sideband has a frequency that is the fundamental frequency plus the modulation frequency and the lower sideband has a frequency that is the fundamental frequency minus the modulation frequency. The energy of the combination is larger than the energy of the unmodulated fundamental.

Figure 1 shows the magnitudes of amplitude modulation sidebands relative to fundamental magnitude of 1. This figure shows the case of amplitude modulation with a 10 Hz modulation frequency and a modulation index of 0.1.

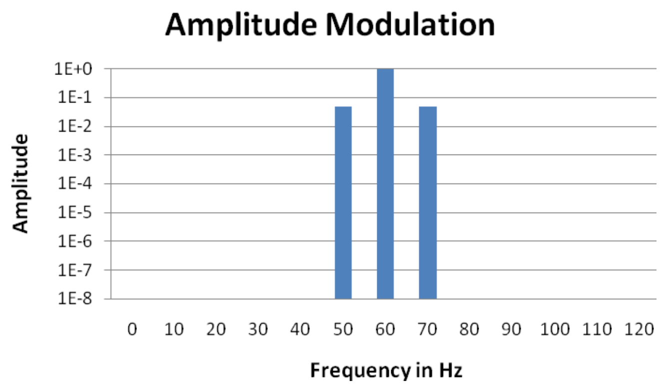

Figure 1. Amplitude modulation sideband magnitudes

B. Phase modulation

The formula for phase modulation is given by

$$X_a = X_m \cos\left[\omega_0\, t + k_a \sin(\omega t + \theta)\right]. \tag{10}$$

Phase modulation gives a family of sidebands with frequencies above and below the fundamental frequency with frequency spacing also equal to the modulation frequency. The sidebands immediately above and below the fundamental are called the first order sidebands. The next sidebands above and below the fundamental are the second order sidebands, etc. For modulation indexes that we are interested in of 0.1 to 0.2, the magnitudes of the sidebands fall off quickly.

A phase modulated signal is given by [23]

$$\begin{aligned} X_a = X_m\big[& \mathrm{J}_0(k_a)\cos(\omega_0\, t) \\ & + \mathrm{J}_1(k_a)\left[\cos[(\omega_0+\omega)t+\theta] - \cos[(\omega_0-\omega)t-\theta]\right] \\ & + \mathrm{J}_2(k_a)\left[\cos[(\omega_0+2\omega)t+2\theta] + \cos[(\omega_0-2\omega)t-2\theta]\right] \\ & + \mathrm{J}_3(k_a)\left[\cos[(\omega_0+3\omega)t+3\theta] - \cos[(\omega_0-3\omega)t-3\theta]\right] \\ & + \cdots\ \big], \end{aligned} \tag{11}$$

where $\mathrm{J}_{\mathrm{n}}(k_a)$ is the n[th] order Bessel function of the first kind. For k_a small (< 0.2) we get the following approximations

$$\begin{aligned} & \mathrm{J}_0(k_a) \cong 1 - \frac{k_a^2}{2^2}, \qquad \mathrm{J}_1(k_a) \cong \frac{k_a}{1!\ 2^1}, \\ & \mathrm{J}_2(k_a) \cong \frac{k_a^2}{2!\ 2^2}, \qquad \mathrm{J}_3(k_a) \cong \frac{k_a^3}{3!\ 2^3}, \quad \text{etc!}. \end{aligned} \tag{12}$$

These approximations show as mentioned above that for k_a small the sidebands drop quickly in magnitude.

Comparing the amplitude and phase modulation equations, one sees that for small phase modulation index k_a equal to the amplitude modulation index k_x the magnitudes of the first order sidebands are approximately equal. However, the lower sidebands have opposite signs. With the sine function in the phase modulation equation (10), equation (11) shows that at time t = 0 the sidebands are either in phase with the fundamental or have the opposite sign. With a cosine function in place of the sine function, some sidebands are perpendicular to the fundamental signal. That is why it is convenient to adopt the sine function for the modulation equation for this analysis.

Figure 2 shows the magnitudes of the many phase modulation sidebands relative to fundamental magnitude 1. This figure shows the case of phase modulation with a 10 Hz modulation frequency and a modulation index of 0.1.

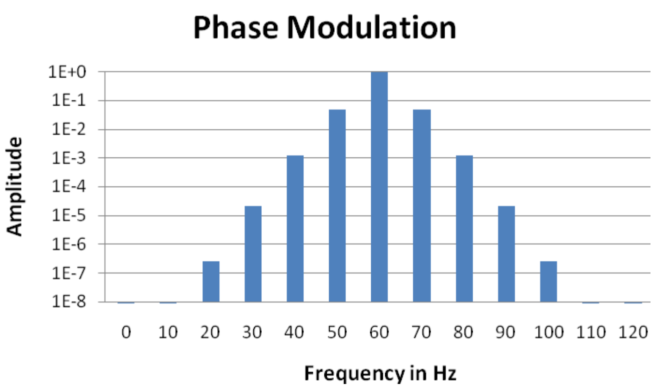

Figure 2. Phase modulation sideband magnitudes

C. *Combined Modulation*

For a combined amplitude and phase modulation it is helpful to use the following view. Consider starting with an amplitude modulated waveform. This has the fundamental and two sidebands. If we phase modulate these three components, each of the three signals will get phase modulated, giving rise to three families of sidebands. We can view this as three phase-modulated signals. This three phase-modulated signals model was used in [22] to analyze the combined modulated signals. This was done with an iterative process to solve for the modulation parameter to fit the data to three phase-modulated signals and amplitude modulation parameters. In this paper we solve for the equations that describe each of the sidebands. Then we use these equations to give a direct solution for the modulation parameters. These modulation parameters can be used to determine the phasors, frequency, and ROCOF values.

One can equally well view the combined modulation as starting with a family of phase-modulated sidebands given by (11). To identify the various components let's use 0 for the fundamental, positive integers for the upper sidebands (1, 2, 3 …), and negative integers for the lower sidebands (-1, -2, -3 …). Looking at an individual component n of the phase-modulated signal, what will the corresponding sideband be for the combined modulated waveform? From the nature of amplitude modulation given in (9) we can see that the corresponding component will be the sum of three vectors. It will be the vector sum of the phase-modulated component n, plus an amplitude-modulated lower sideband from phase-modulation component n+1, and an amplitude-modulated upper sideband from phase-modulation component n-1.

Figure 3 shows the magnitudes of the combined phase and amplitude modulation sidebands relative to fundamental magnitude 1. This figure shows the case of combination phase modulation with a 10 Hz modulation frequency and a modulation index of 0.1 and amplitude modulation with a 10 Hz modulation frequency and a modulation index of 0.1. At each of the sideband locations three magnitudes are plotted. The total sideband at each location is the vector sum of these three components. This plot only shows the magnitudes of the components and not their relative angles. This modulation can be viewed as starting with an amplitude modulation giving a fundamental and two sidebands. This set of three components is then phase modulated. The blue components show the many phase modulation components from phase modulating the fundamental. The red components show the many phase modulation components from phase modulating the amplitude modulation lower sideband. The green components show the many phase modulation components from phase modulating the amplitude modulation upper sideband. Each combined modulation sideband receives a contribution from each of the three components of the amplitude modulation.

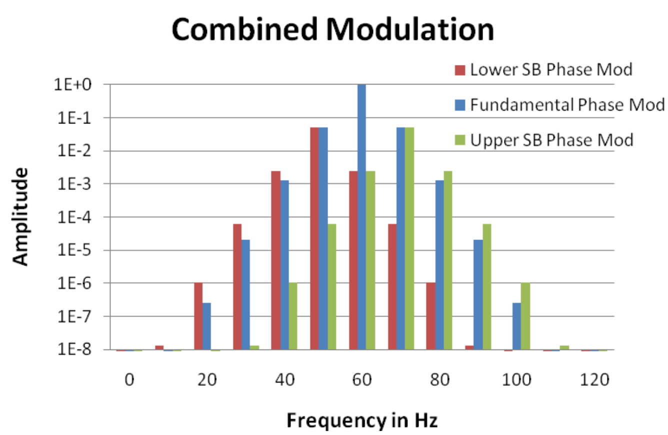

Figure 3. Combined amplitude and phase modulation sideband magnitudes.

In this paper, as stated before, we always assume that the amplitude and phase modulations have the same frequency. The general form of the combined amplitude and phase modulation is given by

$$X_a = X_m\left[1 + k_x \cos(\omega t + \varphi)\right]\cos\left[\omega_0 t + k_a \sin(\omega t + \theta)\right], \quad (13)$$

which is the same as equation (1). From the discussions above of a combined modulation signal, we see that the combination fundamental and each sideband will have contributions from each of the three sine waves in the amplitude modulated signal, or analogously from each of the three phase-modulated signals.

Using the numbering described above the fundamental component is designated as X_{a0}, the first order upper sideband as X_{a1}, and the first order lower sideband as $X_{a\text{-}1}$. Look first at the fundamental component X_{a0} of the combined modulation (13). It is given by

$$X_{a0} = X_m \Big[\mathrm{J}_0(k_a)\cos(\omega_0 t) + \mathrm{J}_1(k_a)\frac{k_x}{2}\left[\cos(\omega_0 t + \varphi - \theta) - \cos(\omega_0 t - \varphi + \theta)\right] \Big]. \quad (14)$$

This can be rewritten as

$$X_{a0} = X_m \left[\mathrm{J}_0(k_a)\cos(\omega_0 t) + \mathrm{J}_1(k_a) k_x \sin(\varphi - \theta)\sin(\omega_0 t) \right]. \quad (15)$$

This can be viewed as a vector equation. It has a component in phase with the fundamental, the $\cos(\omega_0 t)$ term, and a vector component perpendicular to the fundamental, the $\sin(\omega_0 t)$ term. That is how this expression is turned into (7) in section 2 for the fundamental component of a combined modulation at time $t = 0$ as

$$\vec{X}_{a0} = X_m \mathrm{J}_0(k_a)\angle 0 + X_m k_x \mathrm{J}_1(k_a)\sin(\varphi - \theta)\angle -\frac{\pi}{2}. \quad (16)$$

Thus, as mentioned in that section, the magnitude of the combination fundamental is negligibly larger than the phase modulated magnitude. The phase of the fundamental is dependent on the difference between the amplitude and phase modulation angles, φ and θ. For modulation indices of 0.1 this difference can gives a maximum angle change of 0.005 rad or 0.29°. This would represents a TVE of about 0.5% if one had assumed that the phase of the steady-state phasor is the same as the unmodulated phasor. This would be a significant error contribution.

The first order upper sideband of the combined modulation (13) is given by

$$X_{a1} = X_m \Big[\mathrm{J}_1(k_a)\cos[(\omega_0 + \omega)t + \theta] + \mathrm{J}_0(k_a)\frac{k_x}{2}\cos[(\omega_0 + \omega)t + \varphi] + \mathrm{J}_2(k_a)\frac{k_x}{2}\cos[(\omega_0 + \omega)t - \varphi + 2\theta] \Big]. \quad (17)$$

The first order lower sideband of the combined modulation is given by

$$X_{a-1} = X_m \Big[-\mathrm{J}_1(k_a)\cos[(\omega_0 - \omega)t - \theta] + \mathrm{J}_0(k_a)\frac{k_x}{2}\cos[(\omega_0 - \omega)t - \varphi] + \mathrm{J}_2(k_a)\frac{k_x}{2}\cos[(\omega_0 - \omega)t + \varphi - 2\theta] \Big]. \quad (18)$$

The nth order upper sideband of the combined modulation (13) is given by

$$X_{an} = X_m \Big[\mathrm{J}_n(k_a)\cos[(\omega_0 + n\omega)t + n\theta] + \mathrm{J}_{n-1}(k_a)\frac{k_x}{2}\cos[(\omega_0 + n\omega)t + \varphi + (n-1)\theta] + \mathrm{J}_{n+1}(k_a)\frac{k_x}{2}\cos[(\omega_0 + n\omega)t - \varphi + (n+1)\theta] \Big]. \quad (19)$$

The nth order lower sideband of the combined modulation is given by

$$X_{a-n} = X_m \Big[(-1)^n \mathrm{J}_n(k_a)\cos[(\omega_0 - n\omega)t - n\theta] + \mathrm{J}_{n-1}(k_a)\frac{k_x}{2}\cos[(\omega_0 - n\omega)t - \varphi - (n-1)\theta] + \mathrm{J}_{n+1}(k_a)\frac{k_x}{2}\cos[(\omega_0 - n\omega)t + \varphi - (n+1)\theta] \Big]. \quad (20)$$

The form of the sidebands (19) and (20) show the structure outlined above. They each have three components. One is from the phase modulation of the fundamental, the term with the Bessel function order n. Note that for the lower order sidebands this term alternates in sign as n increments. Another term is an amplitude modulated sideband, note coefficient k_x, of the phase modulated term with order n-1. In magnitude this term is of the same order at the first term. Similarly, an amplitude modulation sideband term with Bessel order n+1 and k_x coefficient is from the next higher order phase modulated sideband. In magnitude this term is much smaller than the first two terms.

This gives the equations of the combined modulation signals in terms of the modulation parameters. For validation of PMU calibrators or for calibration of PMU calibrators we need to be able to derive these parameters from measurement of the calibrator output waveforms. Thus, from the measurement of the fundamental waveform and the first two sidebands, the next two sections show how these can be used to derive the modulation parameters. The next section gives approximate solutions and the following section gives more accurate solutions.

V. Approximate Inverse Modulation Equations

The fundamental is a phasor that is rotating near 50 Hz or 60 Hz. The upper sidebands are rotating faster than the fundamental and the lower sidebands are rotating slower. Using a rotating frame of reference that is rotating at the rate of the fundamental, the first order upper sideband appears to be rotating counterclockwise at the modulation frequency. Similarly, the first order lower sideband appears to be rotating clockwise at the modulation frequency. From this perspective we can see that the sum of the upper and lower first order sidebands for pure amplitude modulation gives the modulation magnitude. Similarly, the sum of these two sidebands for a pure phase modulation gives the phase modulation magnitude.

The equation for the sum of the first order sidebands S_{a1} for a combined modulation is given by

$$S_{a1} = X_m \left[-2\mathrm{J}_1(k_a)\sin(\omega_0 t)\sin(\omega t + \theta) + \mathrm{J}_0(k_a) k_x \cos(\omega_0 t)\cos(\omega t + \varphi) + \mathrm{J}_2(k_a) k_x \cos(\omega_0 t)\cos(\omega t - \varphi + 2\theta) \right]. \quad (21)$$

The equation for the lower minus the upper first order sidebands D_{a1} is given by

$$D_{a1} = X_m \left[-2\mathrm{J}_1(k_a)\cos(\omega_0 t)\cos(\omega t + \theta) + \mathrm{J}_0(k_a) k_x \sin(\omega_0 t)\sin(\omega t + \varphi) + \mathrm{J}_2(k_a) k_x \sin(\omega_0 t)\sin(\omega t - \varphi + 2\theta) \right]. \quad (22)$$

For k_a small we can use the approximations given in (12). Neglecting terms of order $\mathrm{J}_1(k_a)\, k_x$ and smaller, (15) can be approximated as $X_{a0} \cong X_m \cos(\omega_0 t)$ and the sum and difference equations are approximately

$$S_{a1} \cong X_m[-k_a \sin(\omega_0 t)\sin(\omega t+\theta) + k_x \cos(\omega_0 t)\cos(\omega t+\varphi)], \quad (23)$$

and

$$D_{a1} \cong X_m[-k_a \cos(\omega_0 t)\cos(\omega t+\theta) + k_x \sin(\omega_0 t)\sin(\omega t+\varphi)]. \quad (24)$$

Both of these can be expressed as the vector sum of a vector parallel to the fundamental, $\cos(\omega_0 t)$ terms, and a vector perpendicular to the fundamental, $\sin(\omega_0 t)$ terms. Thus, in the analysis of the waveforms we can break the sum and difference equations of the first order sidebands into components in parallel with the fundamental and components perpendicular to the fundamental. These can be expressed as

$$\vec{S}_{a1} = \vec{S}_{a1}\perp + \vec{S}_{a1}\| \quad \text{and}$$
$$\vec{D}_{a1} = \vec{D}_{a1}\| + \vec{D}_{a1}\perp . \quad (25)$$

Let the magnitude of the sum component perpendicular to the fundamental be given by $S_{a1}\perp$ and the other component magnitudes indicated by the corresponding name without the vector symbol. From these equations and this nomenclature we can get approximate forms for the modulation parameters from these measured values. These are given by

$$k_a \cong \frac{1}{X_{a0}}\left((S_{a1}\perp)^2 + (D_{a1}\|)^2\right)^{1/2},$$
$$k_x \cong \frac{1}{X_{a0}}\left((S_{a1}\|)^2 + (D_{a1}\perp)^2\right)^{1/2}, \quad (26)$$
$$\theta \cong \arctan\left(\frac{S_{a1}\perp}{D_{a1}\|}\right), \text{ and}$$
$$\varphi \cong \arctan\left(\frac{D_{a1}\perp}{S_{a1}\|}\right).$$

Putting these approximations into (4), (5), and (6) to give phasor, frequency, and ROCOF estimates gives the following results. The phasors have a maximum TVE of about 0.04 %, frequencies have a maximum error of about 0.6 mHz, and ROCOFs have a maximum error of about 3 mHz/s. These are fairly good estimates.

VI. Higher Accuracy Inverse Modulation Equations

Using the full accuracy formulas for the sum and difference of the first order sidebands (21) and (22) gives higher accuracy estimates for the modulation parameters. We can see that the formula for the phase modulation angle θ is not affected by the approximations. The formula for the phase modulation index is actually for twice the first order Bessel function of the modulation index, which is

$$2\,J_1(k_a) = \frac{1}{X_{a0}}\left((S_{a1}\perp)^2 + (D_{a1}\|)^2\right)^{1/2}, \quad (27)$$

Determining the phase modulation index requires the inverse Bessel function. A power series approximation for the first order Bessel function is given by the first terms of a series

$$J_1(k_a) = \frac{k_a}{2} - \frac{k_a^3}{1!\,2!\,2^3} + \frac{k_a^5}{2!\,3!\,2^5} - \cdots . \quad (28)$$

From this equation we can get an inverse first order Bessel function that is good for k_a less than 0.2. It is given by

$$k_a \cong 2\,J_1(k_a) + (J_1(k_a))^3 + 1.356\,(J_1(k_a))^5 . \quad (29)$$

Similarly we can derive formulas for the amplitude modulation terms. The amplitude modulation index is given by

$$k_x = \frac{D_{a1}\perp}{(J_0(k_a)\sin(\varphi) - J_2(k_a)\sin(\varphi - 2\,\theta))}. \quad (30)$$

Let $c_1 = J_0(k_a) - J_2(k_a)\cos(2\,\theta)$, and $c_2 = J_2(k_a)\sin(2\,\theta)$. Then the amplitude modulation phase angle is given by

$$\varphi = \arcsin\left(\frac{D_{a1}\perp c_1 - S_{a1}\| c_2}{k_x\left(J_0(k_a) - (J_2(k_a))^2\right)}\right). \quad (31)$$

Equations (30) and (31) are not independent so must be solved iteratively.

Putting these higher accuracy approximations into (4), (5), and (6) to give phasor, frequency, and ROCOF estimates gives the following results. The phasors have a maximum TVE of about 0.00013 % , frequencies have a maximum error of about 6.3 μHz, and ROCOFs have a maximum error of about 31 μHz/s. These are excellent estimates.

VII. Conclusions

Approximate and higher accuracy equations have been derived for the modulation parameters based on the Fourier components of the modulated signal. By sampling of the modulated signals over one or more cycles of the modulation the Fourier components of the signal can be estimated. These can be used to calculate the modulation parameters and thus the dynamic and steady state phasor values. For the calibration of PMU calibrators such an approach is important to assure that the calibrator is generating the proper estimates for the phasors that it indicates it is producing.

This analysis has shown an unexpected phase shift of the steady state phasor that is dependent on the difference in angle of the phase modulation and the amplitude modulation. For modulation parameters of the order currently being considered by the revised C37.118 standard, this can cause a TVE of as large as 0.5% from an assumption that the steady-state phasors are the same as the unmodulated fundamental phasors.

A complete analysis of the errors in the estimation process will require consideration of the errors in sampling the modulated signal. This will include quantization errors as well as magnitude, timing, and noise errors. The modulation parameters derived from the analysis should be used to solve for the estimated values of the waveform at all sampled times. The mean and maximum differences between the measured and estimated values can be used to estimate the uncertainty of the analysis and how pure the modulated signals are.

VIII. Acknowledgment

The author gratefully acknowledges the contribution of

Ming Zhou for her development of the combined modulation analysis algorithm used in the NIST PMU calibration system. Her method is based on the three phase-modulated waveform method. The author appreciates the significant corrections and improvements from the reviewers.

IX. References

[1] Martin, K.E.; "Phasor measurement systems in the WECC," *Power Engineering Society General Meeting, 2006. IEEE* , vol., no., pp.7.

[2] Novosel, D.; Begovic, M.M.; Madani, V.; , "Shedding light on blackouts," *Power and Energy Magazine, IEEE* , vol.2, no.1, pp. 32- 43, Jan-Feb 2004.

[3] Taylor, C.W.; Erickson, D.C.; Martin, K.E.; Wilson, R.E.; Venkatasubramanian, V.; "WACS-Wide-Area Stability and Voltage Control System: R&D and Online Demonstration," *Proceedings of the IEEE* , vol.93, no.5, pp.892-906, May 2005.

[4] Hauer, J.F.; Mittelstadt, W.A.; Martin, K.E.; Burns, J.W.; Lee, H.; Pierre, J.W.; Trudnowski, D.J.; "Use of the WECC WAMS in Wide-Area Probing Tests for Validation of System Performance and Modeling," *Power Systems, IEEE Transactions on* , vol.24, no.1, pp.250-257, Feb. 2009.

[5] de la O Serna, J.A.; "Dynamic Phasor Estimates for Power System Oscillations and Transient Detection," IEEE Power Engineering Society General Meeting, 2006, 18-22 June 2006, 7 p.

[6] de la O Serna, J.A.; Martin, K.E.; "Improving phasor measurements under power system oscillations," *Power Systems, IEEE Transactions on* , vol.18, no.1, pp. 160- 166, Feb 2003.

[7] Zhou, N.; Trudnowski, D.; Pierre, J.W.; Sarawgi, S.; Bhatt, N.; "An algorithm for removing trends from power-system oscillation data," *Power and Energy Society General Meeting - Conversion and Delivery of Electrical Energy in the 21st Century, 2008 IEEE* , vol., no., pp.1-7, 20-24 July 2008.

[8] Zhenyu Huang; Ning Zhou; Tuffner, F.; Yousu Chen; Trudnowski, D.; Mittelstadt, W.; Hauer, J.; Dagle, J.; "Improving small signal stability through operating point adjustment," *Power and Energy Society General Meeting, 2010 IEEE* , vol., no., pp.1-8, 25-29 July 2010.

[9] Trudnowski, D.J.; Pierre, J.W.; "Overview of algorithms for estimating swing modes from measured responses," *Power & Energy Society General Meeting, 2009. PES '09. IEEE* , vol., no., pp.1-8, 26-30 July 2009.

[10] IEEE Standard for Synchrophasors for Power Systems, IEEE Standard PC37.118-2005.

[11] Martin, K.E.; Hamai, D.; Adamiak, M.G.; Anderson, S.; Begovic, M.; Benmouyal, G.; Brunello, G.; Burger, J.; Cai, J.Y.; Dickerson, B.; Gharpure, V.; Kennedy, B.; Karlsson, D.; Phadke, A.G.; Salj, J.; Skendzic, V.; Sperr, J.; Song, Y.; Huntley, C.; Kasztenny, B.; Price, E.; "Exploring the IEEE Standard C37.118–2005 Synchrophasors for Power Systems," *Power Delivery, IEEE Transactions on* , vol.23, no.4, pp.1805-1811, Oct. 2008.

[12] Martin, K. E.; "Synchrophasors in the IEEE C37.118 and IEC 61850," *Critical Infrastructure (CRIS), 2010 5th International Conference on* , vol., no., pp.1-8, 20-22 Sept. 2010.

[13] Yang, G. Y.; Martin, K. E.; Ostergaard, J.; "Investigation of PMU Performance Under TVE criterion," *Critical Infrastructure (CRIS), 2010 5th International Conference on* , vol., no., pp.1-7, 20-22 Sept. 2010.

[14] Zhenyu Huang; Kasztenny, B.; Madani, V.; Martin, K.; Meliopoulos, S.; Novosel, D.; Stenbakken, J.; "Performance evaluation of phasor measurement systems," *Power and Energy Society General Meeting - Conversion and Delivery of Electrical Energy in the 21st Century, 2008 IEEE* , vol., no., pp.1-7, 20-24 July 2008.

[15] Meliopoulos, A.P.S.; Cokkinides, G.J.; Hedrington, C.; Conrad, T.L.; "The supercalibrator — A fully distributed state estimator," *Power and Energy Society General Meeting, 2010 IEEE* , vol., no., pp.1-8, 25-29 July 2010.

[16] Martin, K.E.; Hauer, J.F.; Faris, T.J.; , "PMU Testing and Installation Considerations at the Bonneville Power Administration," *Power Engineering Society General Meeting, 2007. IEEE* , vol., no., pp.1-6, 24-28 June 2007.

[17] Phadke, A.G.; Kasztenny, B.; "Synchronized Phasor and Frequency Measurement Under Transient Conditions," *Power Delivery, IEEE Transactions on* , vol.24, no.1, pp.89-95, Jan. 2009.

[18] Zhenyu Huang; Hauer, J.F.; Martin, K.E.; "Evaluation of PMU Dynamic Performance in Both Lab Environments and under Field Operating Conditions," *Power Engineering Society General Meeting, 2007. IEEE* , vol., no., pp.1-6, 24-28 June 2007.

[19] Yi Hu; Novosel, D.; "Progresses in PMU testing and calibration," *Electric Utility Deregulation and Restructuring and Power Technologies, 2008. DRPT 2008. Third International Conference on* , vol., no., pp.150-155, 6-9 April 2008.

[20] Stenbakken, G.N.; Ming Zhou; "Dynamic Phasor Measurement Unit Test System," IEEE Power Engineering Society General Meeting, 2007, 24-28 June 2007, 8 p.

[21] Premerlani, W.; Kasztenny, B.; and Adamiak, M.; "Development and Implementation of a Synchrophasor Estimator Capable of Measurements Under Dynamic Conditions", IEEE Transactions on Power Delivery, Volume: 23, Issue: 1, pp 109 – 123 Jan 2008.

[22] Stenbakken, G.; Nelson, T.; Ming Zhou; Centeno, V.; "Reference Values for Dynamic Calibration of PMUs," *Hawaii International Conference on System Sciences, Proceedings of the 41st Annual* , Issue 7, pp.171, 6 p., 10 Jan. 2008.

[23] Hewlett Packard Test &Measurement Application Note 150-1, "Spectrum Analysis Amplitude and Frequency Modulation," available at http://www.tm.agilent.com/data/static/downloads/eng/Notes/interactive/an-150-1/hp-am-fm.pdf .

X. Biography

Gerard Stenbakken (M'71) received his B. of Physics from the University of Minnesota in 1964, the M.S. in Physics and the M.S. in electrical engineering from the University of Maryland in 1969 and 1986, respectively. He started working at Vitro Laboratories in 1963 and moved to the National Bureau of Standards (now the National Institute of Standards and Technology) in 1969. His areas of interest include electric power metrology, semiconductor measurements, sampling metrology, testing strategies, and magnetic field modeling. He formed GNS Consulting in 2009 for research in power metrology.